J|A|C|S
COMMUNICATIONS

Published on Web 09/06/2003

Resolution Enhancement in Multidimensional Solid-State NMR Spectroscopy of Proteins Using Spin-State Selection

Luminita Duma,[†] Sabine Hediger,*[,†] Bernhard Brutscher,[‡] Anja Böckmann,[§] and Lyndon Emsley*[,†]

Laboratoire de Chimie, UMR 5532 CNRS/ENS, Ecole Normale Supérieure de Lyon, 69364 Lyon, France, Institut de Biologie Structurale Jean-Pierre Ebel CNRS/CEA, 38027 Grenoble, France, and Institut de Biologie et Chimie des Protéines, UMR 5086 CNRS, 69367 Lyon, France

Received June 25, 2003; E-mail: sabine.hediger@ens-lyon.fr; lyndon.emsley@ens-lyon.fr

Much progress has recently been made in the field of solid-state NMR of isotope (^{13}C, ^{15}N)-enriched biomolecules, leading to the first protein structure solved by solid-state NMR.[1] One of the principal factors limiting the study of larger systems remains spectral resolution. In uniformly ^{13}C-labeled compounds such as proteins, the ^{13}C−^{13}C *J*-couplings constitute a significant contribution to the line width in magic-angle-spinning (MAS) spectra. *J*-decoupling techniques for solid-state NMR using semiselective pulses were first proposed in 1996 by Straus et al.[2] to enhance the spectral resolution in indirectly detected spectral dimensions. Here, we present the application of spin-state selective and transition-selective polarization transfer to multidimensional solid-state NMR correlation experiments of ^{13}C-labeled proteins. We show that single-transition selection removes the line broadening due to the $J_{COC\alpha}$ spin coupling in both direct and indirect dimensions of a two-dimensional CO−C$^{\alpha}$ correlation experiment. A nearly two-fold improvement in line width is thus obtained on a sample of microcrystalline Crh, an 85-residue protein involved in carbon catabolite repression in *Bacillus subtilis*, for which solid-state NMR chemical shifts have recently been assigned.[3]

Spin-state-selective NMR techniques have been developed in liquid-state NMR spectroscopy for the measurement of small spin−spin coupling constants and for transverse-relaxation-optimized spectroscopy (TROSY).[4] Recently, we have demonstrated the feasibility of homonuclear spin-state selection in the solid state,[5] even for *J*-couplings that are not resolved, using an in−phase-anti-phase (IPAP)-type selection filter.[6] To perform a multidimensional experiment, the selected transition of the first spin, *I*, evolving during t_1 should be transferred to a single-transition of a second spin, *S*, by means of an appropriate mixing sequence. Generally, spin-state-selective coherence transfer is obtained through zero-quantum (ZQ) or double-quantum (DQ) rotations.[7] A ZQ rotation "conserves" the spin state ($I_xS^{\alpha} \rightarrow I^{\alpha}S_x$), and a DQ rotation "reverses" the spin state ($I_xS^{\alpha} \rightarrow I^{\beta}S_x$). In liquid-state NMR, spin-state-selective coherence transfer is obtained using planar mixing or S^{3}CT building blocks.[8] Similar *J*-based spin-state-selective transfer techniques could be envisaged in the solid state. However, schemes using the dipolar coupling may be more appropriate for solid-state applications since most of the (many) existing solid-state dipolar correlation techniques under MAS have a ZQ or DQ average Hamiltonian, and may therefore be used directly for spin-state-selective polarization or coherence transfer. Common examples of such sequences are proton-driven spin diffusion (PDSD)[9] and RFDR,[10] with a ZQ-average Hamiltonian, and C7, POST-C7, and SPC5 with a DQ-average Hamiltonian.[11]

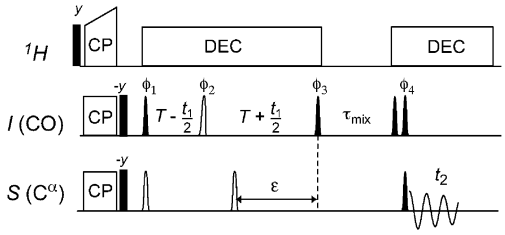

Figure 1. Pulse sequence suitable for an *I*−*S* (e.g., CO−C$^{\alpha}$) correlation experiment; 90° and 180° rf pulses are represented by filled and open bars, respectively. The CO pulses are applied with the shape of the center lobe of a (sin *x*)/*x* function, whereas the C$^{\alpha}$ pulses were rectangular with $\omega_1 = \Delta/\sqrt{15}$ (90°) and $\Delta/\sqrt{3}$ (180°), where Δ is the difference in Hz between the centers of the CO and C$^{\alpha}$ spectral regions. All pulses are applied along the *x* axis unless indicated. An eight-step phase cycle was applied with $\phi_1 = 4x, 4(-x)$; $\phi_2 = x, y, -x, -y$; $\phi_{rec} = x, -x, x, -x, -x, x, -x, x$. The constant time delay $2T$ is adjusted to $(2J_{COC\alpha})^{-1}$. Four data sets (A1), (A2), (B1), and (B2) are recorded. A- and B-type experiments are used to separate the *I*-spin transitions using IPAP with the following settings: (A) $\epsilon = 0$, $\phi_3 = -x$ and (B) $\epsilon = T$, $\phi_3 = y$. Each of the experiments A and B are recorded twice by setting alternatively the phase ϕ_4 to *x* and $-x$. Addition of the two data sets yields in-phase spectra in ω_2 (A1, B1), subtraction yields spectra anti-phase in ω_2 (A2, B2). Linear combinations (A1 + δB1) ± *k*(A2 + δB2) yield the four different single-transition correlation spectra (αα, α*β*, *β*α, *ββ*) with $\delta = +1$ or -1 and *k* a scaling factor taking into account the different PDSD transfer amplitudes. The pulse sequence is available from our website[13] or upon request.

The pulse sequence shown in Figure 1 yields a spin-state-selective CO−C$^{\alpha}$ correlation experiment using PDSD. After cross-polarization, both *I* (CO) transitions are separated into different subspectra with respect to the *S* (C$^{\alpha}$) spin by an IPAP sequence. The t_1 period is built into the IPAP sequence, providing a constant time (CT) experiment.[12] PDSD then yields spin-state-selective CO → C$^{\alpha}$ polarization transfer. During the PDSD mixing period, CO polarization (I_z) is transferred to C$^{\alpha}$ polarization (S_z) by the dipolar coupling, but the two-spin order $2I_zS_z$, present after t_1 evolution, is not affected by the dipolar coupling. Since the build-up of S_z and the decay of $2I_zS_z$ depend differently on the mixing time τ_{mix}, and to obtain proper spin-state selection independent of τ_{mix}, the two polarization-transfer pathways are separated into different subspectra by an appropriate two-step phase cycle, as detailed in the caption of Figure 1. By separating the in-phase and anti-phase components of the *S*-spin coherence during detection (t_2), their relative amplitude can be adjusted by an appropriate scaling factor, *k*, to yield proper spin-state selection.

Figure 2 shows the (αα)-subspectrum recorded for a microcrystalline sample of uniformly ^{13}C−^{15}N-labeled Crh using the sequence of Figure 1, compared to a standard PDSD correlation spectrum. Spin-state selection provides a remarkable increase in resolution in both dimensions. Specifically, the line width of the Gly49 cross-peak is enhanced by 44 and 17% for C$^{\alpha}$ and CO

[†] Laboratoire de Chimie, UMR 5532 CNRS/ENS, Ecole Normale Supérieure de Lyon.
[‡] Institut de Biologie Structurale Jean-Pierre Ebel CNRS/CEA.
[§] Institut de Biologie et Chimie des Protéines, UMR 5086 CNRS.

10.1021/ja036893n CCC: $25.00

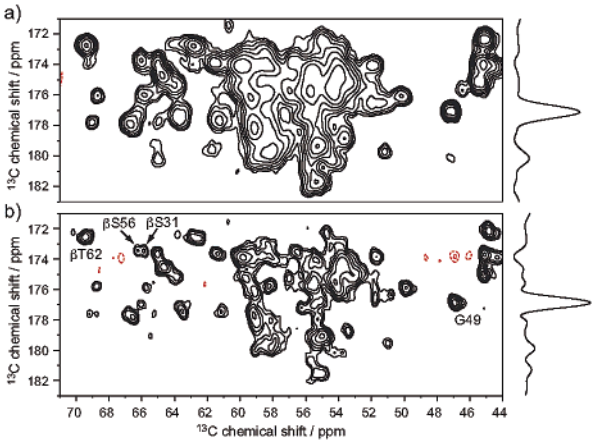

Figure 2. CO−C$^{\alpha}$ region of the standard (a) and the ($\alpha\alpha$)-spin-state-selective (b) PDSD spectrum of microcrystalline Crh. The second spectrum was obtained from the linear combination A1 + B1 + k(A2 + B2), with $k = 0.7$. Columns (normalized) are shown for each spectrum through the G49 resonance. Both experiments were performed on a Bruker Avance spectrometer operating at a ^{1}H frequency of 500.13 MHz with a 4 mm double-resonance CP/MAS probe. The temperature was set to 269 K, and the MAS frequency was 11 kHz. CP contact time was 1.8 ms. SPINAL[16] ^{1}H decoupling was used with $\omega_1 = 78$ kHz. τ_{mix} was 30 ms. Acquisition times $t_1^{max} = 9.2$ ms with States quadrature detection and $t_2^{max} = 25$ ms were used. The experimental time was 26 h and 4 × 10 h for the standard and the spin-state-selective spectra, respectively. Cosine apodization was applied in both dimensions prior to Fourier transformation. For both spectra, the first contour level was set to 15% of the intensity of the Gly49 resonance, with a factor of 1.4 between levels. Cross-peaks discussed in the text are annotated in (b).

dimensions, respectively. The resolution enhancement is more pronounced in the C$^{\alpha}$ dimension because of the longer acquisition time used for direct detection. Note that because the ^{13}C line widths in solid-state NMR are dominated by refocusable interactions,[14,15] CT experiments do not provide a significant increase in resolution. However, the insertion of t_1 evolution into the IPAP block allows a shortening of the sequence, and thus in this case the use of a CT sequence yields improved sensitivity.

The efficiency of the spin-state-selective experiment compared to the standard PDSD experiment was estimated from measured cross-peak amplitudes to be about 65%. The loss is mainly due to the $2T = 9.2$ ms delay in the IPAP filter (under these conditions about 20% of the carboxyl magnetization is lost during a 9.2 ms simple spin−echo experiment).[5] As we have shown recently,[5,15] this signal loss is greatly reduced by using high-power ^{1}H decoupling during the filter delay and faster spinning of the sample. This is possible for protein samples if a powerful cooling system is available.[17] In addition, the four subspectra can be added after appropriate shifting of the spectrum by $\pm J_{COC\alpha}/2 \approx 27$ Hz along the CO or C$^{\alpha}$ dimensions, resulting in an additional gain of a factor of 2 in signal-to-noise (leading for the Crh spectra here to an overall sensitivity improvement of 30% relative to the PDSD spectrum). We thus expect the spin-state-selective experiment to yield substantially improved sensitivity for an optimized experimental setup.

Figure 3 illustrates how the recorded 2D data sets are combined. The linear combinations (A1 + δ × B1) ± k × (A2 + δ × B2), with $\delta = \pm 1$ and k an adjustable scaling factor, yield all four single-transition-to-single-transition correlation spectra ($\alpha\alpha$), ($\alpha\beta$), ($\beta\alpha$), and ($\beta\beta$). For PDSD mixing times of $\tau_{mix} = 30$ ms and $\tau_{mix} = 15$ ms, the scaling factor was found to be $k = 0.7$ and $k = 0.5$, respectively.

At longer PDSD mixing times some polarization is transferred from the CO to other side-chain carbons (C$^{\beta}$, C$^{\gamma}$, C$^{\delta}$). Since there is no direct scalar coupling between these carbons, there is no

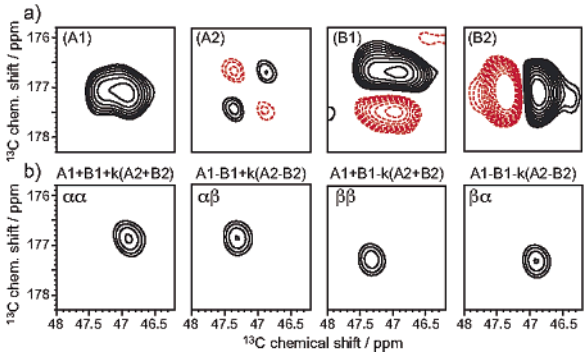

Figure 3. (a) Sub-spectra (A1), (A2), (B1), and (B2) recorded using the spin-state-selective CO−C$^{\alpha}$-PDSD experiment of Figure 1. Experimental details are given in the caption of Figure 2. (b) Separation of the four cross-peak transitions obtained by linear combination of the spectra in (a). For clarity, only the Gly49 cross-peak region is shown. Contours are drawn at the same levels for all spectra.

frequency shift along the detection dimension (ω_2) between the ($\alpha\alpha$) and ($\alpha\beta$), or ($\beta\alpha$) and ($\beta\beta$) subspectra. Thus, the new experiment provides a simple way of distinguishing C$^{\alpha}$ from side-chain carbons (e.g. C$^{\beta}$ of Thr and Ser residues as T62, S31, S56) by comparison of subspectra.

In conclusion, we have introduced a new experimental approach which provides significant resolution enhancement in multidimensional solid-state NMR correlation experiments. Resolution enhancement is achieved by using transition-selective excitation and transfer techniques. Spin-state-selective polarization transfer is obtained using standard ZQ solid-state NMR mixing sequences. Similar results are expected for transfer sequences based on DQ rotations. The new experiment can be easily extended to higher-dimensional experiments. In addition, spin-state-selective correlation experiments allow the distinction of "direct" transfer peaks, involving covalently bound nuclei, and "relayed" transfer peaks. The new experiment is robust and very sensitive. It is expected to become widespread in solid-state NMR of proteins.

References

(1) Castellani, F.; van Rossum, B.; Diehl, A.; Schubert, M.; Rehbein, K.; Oschkinat, H. *Nature* **2002**, *420*, 98.
(2) Straus, S. K.; Bremi, T.; Ernst, R. R. *Chem. Phys. Lett.* **1996**, *262*, 709.
(3) Böckmann, A.; Lange, A.; Galinier, A.; Luca, S.; Giraud, N.; Juy, M.; Heise, H.; Montserret, R.; Penin, F.; Baldus, M. *J. Biomol. NMR* **2003**. In press.
(4) Pervushin, K.; Riek, R.; Wider, G.; Wüthrich, K. *Proc. Natl. Acad. Sci. U.S.A.* **1997**, *94*, 12366.
(5) Duma, L.; Hediger, S.; Lesage, A.; Emsley, L. *J. Magn. Reson.* **2003**, *164*, 187.
(6) (a) Ottiger, M.; Delaglio, F.; Marquardt, J. L.; Tjandra, N.; Bax, A. *J. Magn. Reson.* **1998**, *134*, 365. (b) Andersson, P.; Weigelt, J.; Otting, G. *J. Biomol. NMR* **1998**, *12*, 435.
(7) Meissner, A.; Duus, J. O.; Sørensen, O. W. *J. Biomol. NMR* **1997**, *10*, 89.
(8) Sørensen, M. D.; Meissner, A.; Sørensen, O. W. *J. Biomol. NMR* **1997**, *10*, 181.
(9) Bloembergen, N. *Physica* **1949**, *15*, 386.
(10) Bennett, A. E.; Oak, J. H.; Griffin, R. G.; Vega, S. *J. Chem. Phys.* **1992**, *96*, 8624.
(11) (a) Lee, Y. K.; Kurur, N. D.; Helmle, M.; Johannessen, O. G.; Nielsen, N. C.; Levitt, M. H. *Chem. Phys. Lett.* **1995**, *242*, 304. (b) Hohwy, M.; Jakobsen, H. J.; Eden, M.; Levitt, M. H.; Nielsen, N. C. *J. Chem. Phys.* **1998**, *108*, 2686. (c) Hohwy, M.; Rienstra, C. M.; Jaroniec, C. P.; Griffin, R. G. *J. Chem. Phys.* **1999**, *110*, 7983.
(12) Bax, A.; Mehlkopf, A. F.; Smidt, J. *J. Magn. Reson.* **1979**, *35*, 167.
(13) http://www.ens-lyon.fr/STIM/NMR.
(14) Lesage, A.; Bardet, M.; Emsley, L. *J. Am. Chem. Soc.* **1999**, *121*, 10987.
(15) De Paëpe, G.; Lesage, A.; Emsley, L. *J. Chem. Phys.* **2003**, *119*, 4833.
(16) Fung, B. M.; Khitrin, A. K.; Ermolaev, K. *J. Magn. Reson.* **2000**, *142*, 97.
(17) Ernst, M.; Detken, A.; Meier, B. H.; Böckmann, A. 44th Experimental Nuclear Magnetic Conference, Savannah, Georgia, U.S.A., 2003.

JA036893N